JOURNAL OF THE AMERICAN WATER RESOURCES ASSOCIATION

Vol. 57, No. 5 AMERICAN WATER RESOURCES ASSOCIATION October 2021

A Multiyear Assessment of Irrigation Cooling Capacity in Agricultural and Urban Settings of Central Arizona

Zhaocheng Wang, Enrique R. Vivoni, Theodore J. Bohn, and Zhi-Hua Wang

Research Impact Statement: Remotely-sensed vegetation datasets are used in a high-resolution land surface model evaluated with land surface temperature to assess the spatiotemporal variations of irrigation cooling capacity.

ABSTRACT: Irrigation water use associated with agricultural activities and urban green spaces provides substantial cooling effects and ameliorates heat in central Arizona. In this arid and semiarid area, evaluating the effect of irrigation on land surface temperature (LST) for different types of land use can improve decision making related to water resources management. In this work, we improved the simulation of urban and agricultural irrigation in the Variable Infiltration Capacity model through remotely sensed vegetation and irrigation parameters applied at high spatiotemporal resolution. We then conducted a multiyear (2004–2013) assessment of simulated LST with respect to ground observations and remotely sensed products finding overall good agreement. Overall, results show that irrigation of about 2 mm/day is required to reduce average daily LST by 1°C across the region. Numerical experiments with the validated model also reveal that irrigation leads to LST reductions of higher magnitude and greater spatial variability in croplands than in urban areas. Furthermore, we found that the role of interannual variations in cropping practices is more critical than year-to-year differences in climatic conditions for the evaluation of irrigation cooling capacity. Thus, remotely sensed vegetation products can serve a valuable purpose in quantifying LST reductions and irrigation requirements to achieve a target of heat amelioration.

(KEYWORDS: VIC; land surface temperature; irrigation; urban heat; remote sensing; MODIS.)

INTRODUCTION

Water is a valuable and scarce resource in arid and semiarid regions. The rise of Phoenix in central Arizona, from a set of small agricultural towns into a major metropolitan area, was possible due to complex infrastructure systems that deliver water from upstream watersheds and local aquifers (Sheridan and Luckingham 1990; Gober 2006). With the supply of imported and local water, irrigation in agricultural fields and urban landscaping has proliferated in Phoenix to support food and fiber production, economic development, and municipal water use (Jenerette et al. 2011; Kerna and Frisvold 2014; Rushforth and Ruddell 2015). Aside from its principal use to support crop production and maintain urban vegetation, irrigation has a significant cooling effect through its impact on evaporation, which can ameliorate the elevated temperatures experienced in Phoenix (Georgescu et al. 2008; Song and Wang 2016; Vivoni et al. 2020).

Irrigation water supply is typically limited under the arid conditions of the region and is sensitive to land cover change and climate variations (Gober and

Special Issue: "Use of NASA and other datasets and tools to support water management" Feb 15, 2021. Received June 29, 2020; accepted April 18, 2021. Paper No. JAWR-20-0080-P of the *Journal of the American Water Resources Association* (JAWR).

School of Sustainable Engineering and the Built Environment (Wang, Vivoni, Bohn, Wang), Arizona State University Tempe, Arizona, USA; School of Earth and Space Exploration (Vivoni), Arizona State University Tempe, Arizona, USA; and WattIQ Inc. (Bohn), Honolulu, Hawaii, USA (Correspondence to Vivoni: vivoni@asu.edu).

Citation: Wang, Z., E.R. Vivoni, T.J. Bohn, and Z.-H. Wang. 2021. "A Multiyear Assessment of Irrigation Cooling Capacity in Agricultural and Urban Settings of Central Arizona." *Journal of the American Water Resources Association* 57 (5): 771–788. https://doi.org/10.1111/1752-1688.12920.

Kirkwood 2010; Simonit et al. 2015). In addition, municipal water demand, which is correlated with summer temperature (Balling et al. 2008; Opalinski et al. 2020), may also increase in a warmer future. As a result of increasing water stress, local land planners and water managers have a difficult choice with respect to using urban irrigation as a heat mitigation strategy (e.g., Chow et al. 2012; Gober et al. 2012). It is thus important to understand the tradeoffs between irrigation water use and heat amelioration, referred to here as irrigation cooling efficiency. This topic has received attention previously in Phoenix. For example, Yang and Wang (2017) found that adopting low water use landscaping in urban areas can lead to a reduction of 20% of the annual water demand projected in Phoenix by 2050 but at the expense of increasing urban temperatures by ~1°C.

Irrigation cooling efficiency can be quantified through high-resolution modeling systems that integrate remote sensing products capturing the spatiotemporal variations of irrigation features (Thenkabail et al. 2012; Liu et al. 2021). In central Arizona, there are many cloud-free days that foster the use of remote sensing data. Furthermore, a high contrast exists between irrigated areas and surrounding arid landscapes, facilitating their identification (Ko et al. 2016). Remotely sensed vegetation indices and crop-specific land use datasets have shown promise in arid and semiarid regions for detecting irrigation extents, vegetation types, and crop phenology (Ozdogan and Gutman 2008; Fan et al. 2014; Li, Myint, et al. 2014; Xie et al. 2019). These products have also been used to parameterize the spatiotemporal variations of irrigation extent in land surface models (LSMs) and simulate the effects of irrigation on the water and energy balance. For example, Bohn and Vivoni (2016) incorporated temporal variations in vegetation parameters and planted and irrigated areas in an LSM model. Previous coupled land-atmosphere modeling studies have also shown improvements in urban irrigation simulations when parameterized with satellite observations of green vegetation fraction and albedo (ALB) (Vahmani and Ban-Weiss 2016).

Remote sensing products offer the opportunity to evaluate the performance of high-resolution modeling systems such as LSMs. Land surface temperature (LST), for example, has received attention for its use in the study of the impact of irrigation on surface conditions (Navarro-Estupiñan et al. 2019; Shah et al. 2019; Thiery et al. 2020; Yang et al. 2020). The rich spatiotemporal patterns of LST have also been used to rigorously test simulations in areas with complex terrain and vegetation conditions (Xiang et al. 2014; Ko et al. 2019). Agricultural and urban areas under irrigation exhibit large changes in LST relative to their surrounding natural environments due to the impact of increased soil moisture on the partitioning of available energy. An increase in latent heat flux or evapotranspiration (ET) typically leads to a reduction in LST as energy is consumed for the vaporization of liquid water instead of increasing surface temperatures (Vahmani and Hogue 2014; Wang et al. 2019). Unfortunately, previous studies using remote sensing observations of LST to test high-resolution modeling systems have been limited to short periods or low numbers of scenes that are inadequate to capture the spatiotemporal variations in irrigation and cropping practices.

In this study, we quantify the irrigation cooling efficiency of agricultural and urban areas in central Arizona to support decision making on the tradeoffs between irrigation water use and heat amelioration. To do so, we use ground-based observations and remote sensing products to test the performance of the Variable Infiltration Capacity (VIC) model used to simulate the spatiotemporal patterns of LST. We first improve the representation of irrigation in the model (Bohn and Vivoni 2016) by implementing VIC at a high spatiotemporal resolution (1 km, one hour) and by incorporating time-varying vegetation parameters, crop maps, and irrigation fractions from several remote sensing products. We then conduct a multiyear assessment (2004–2013) of the model capabilities to simulate LST in agricultural, urban, and natural ecosystems through comparisons to observations from the Moderate Resolution Imaging Spectroradiometer (MODIS) and the Geostationary Operational Environmental Satellite (GOES) platforms. Lastly, we utilize the high-resolution modeling system to evaluate the cooling effect of irrigation and the influence of time-varying vegetation and climatic conditions. The irrigation cooling efficiency is evaluated via a new metric, the irrigation cooling capacity (ICC) of Wang et al. (2019, hereafter W19), which is defined as the amount of irrigation water required to reduce LST by 1°C.

STUDY AREA AND DATASETS

Climate and Land Cover Properties

The study region is bounded by 32.50° and 34.00°N latitude and 112.94° and 111.44°W longitude in central Arizona (Figure 1), encompassing two Active Management Areas (AMAs) designated for groundwater administration (Higdon and Thompson 1980). The Phoenix AMA includes urban zones in the Phoenix metropolitan area (PMA) surrounded by agricultural fields and natural areas, while the Pinal AMA

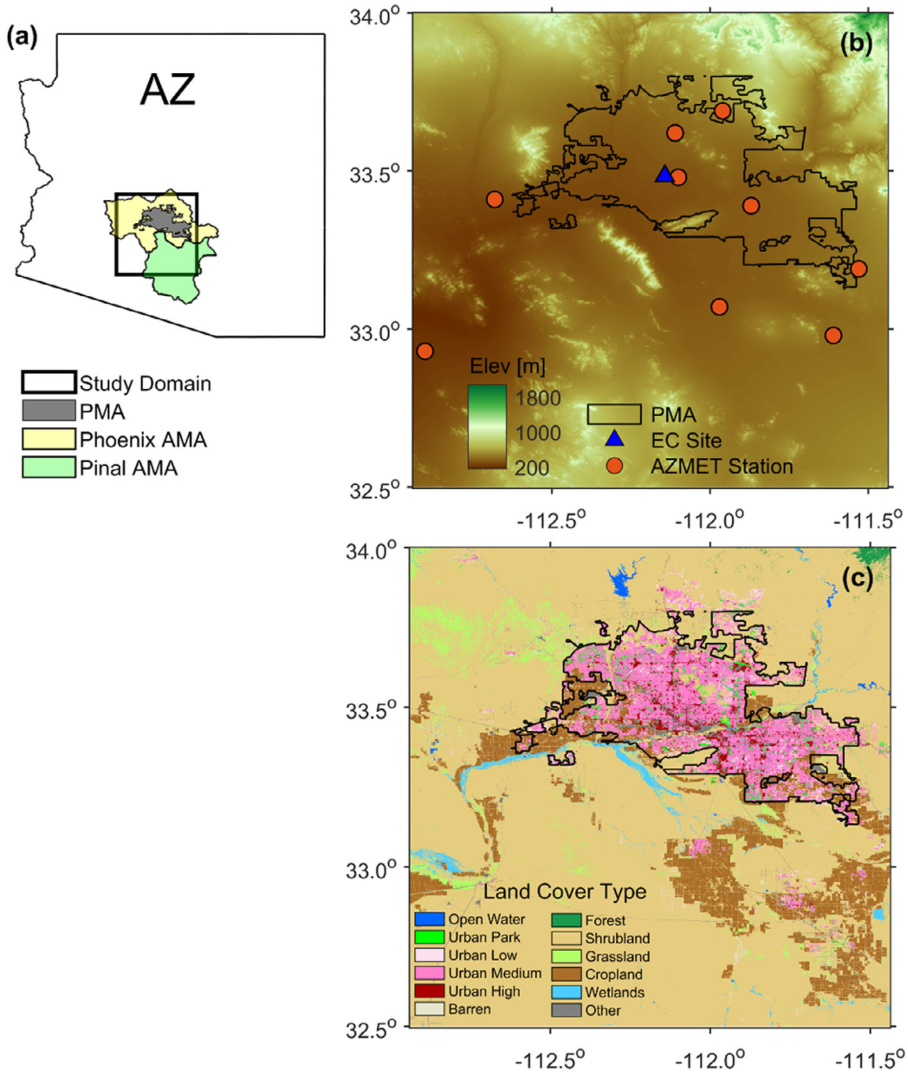

FIGURE 1. (a) Location of the study area and Active Management Areas (AMAs) in central Arizona. (b) Digital elevation model at 30 m resolution from National Elevation Dataset, with locations of meteorological stations from Arizona Meteorological Network (AZMET) (9 in total). (c) Land cover classification at 30 m resolution merged from the National Land Cover Database (NLCD) of 2011 (Homer et al. 2015) and the National Land Use Dataset (NLUD) of 2010 (Theobald 2014) for classes defined in Table 1. PMA, Phoenix metropolitan area; EC, eddy covariance.

includes mostly agricultural fields and the natural ecosystems of the region (e.g., shrublands, grasslands). Located in the Sonoran Desert, central Arizona has a hot, arid climate (Köppen classification BWh), with a mean annual temperature of 24°C and a mean annual precipitation of 204 mm per year according to the 1981–2010 climate normal at Phoenix Sky Harbor International Airport. The precipitation regime is bimodal with the winter (December–February) and summer (July–September) seasons having average amounts of 68.3 and 67.8 mm, respectively (Templeton et al. 2018). Due to the aridity of the region, urban plants and crops require irrigation water that is available from a number of sources including the Colorado, Salt, and Verde Rivers as well as local groundwater wells (Hirt et al. 2008). Seasonality in precipitation and irrigation input induces changes in vegetation that are expected to vary between urban, cropland, and natural ecosystems (Table 1).

Ground Observations and Meteorological Forcing Products

We assembled multiple ground-based and remotely sensed observations to characterize the study region, provide model forcing, and evaluate the high-resolution simulations. Direct estimates of daily ET and longwave radiation were obtained from an eddy

TABLE 1. Percentage (A_f) of land cover and soil texture classes in the study area.

Land cover class	A_f (%)	Soil texture class	A_f (%)
Open water	0.30	Sandy loam	49.37
Urban park	2.32	Loam	44.84
Urban low	5.94	Sandy clay loam	5.30
Urban medium	6.98	Clay loam	0.26
Urban high	1.02		
Barren	0.11		
Forest	0.24		
Shrubland	67.30		
Grassland	1.95		
Cropland	8.04		
Wetlands	0.91		
Other	2.51		

covariance (EC) tower in the neighborhood of Maryvale, Phoenix (Chow et al. 2014), maintained by the Central Arizona–Phoenix Long-Term Ecological Research (CAP-LTER). The turbulent flux footprint of the EC tower consists of impervious surface (48.4%), bare soil (36.8%), and vegetation (14.6%). Additional details of the footprint analysis and the energy balance closure are documented in Chow et al. (2014). We used long-term observations from the Arizona Meteorological Network (AZMET) for the purpose of validating and bias-correcting meteorological forcing products. Table 2 presents the characteristics of the AZMET stations and EC tower, including the years with available data from 2004 to 2013. While other EC measurements are available in Phoenix (Templeton et al. 2018; Perez-Ruiz et al. 2020; Vivoni et al. 2020), their time periods do not coincide with the availability of the gridded meteorological forcing from Livneh et al. (2015) ending in 2013. From the EC measurements, we obtained an in situ LST estimate using:

$$\mathrm{LST} = \left[\frac{L_{\uparrow} - (1-\varepsilon)\cdot L_{\downarrow}}{\varepsilon \cdot \sigma}\right]^{\frac{1}{4}}, \tag{1}$$

where $L_{\uparrow}$ and $L_{\downarrow}$ are the upward and downward longwave radiations, ϵ is the surface emissivity retrieved from MODIS, and σ is the Stefan–Boltzmann constant (5.67×10^{-8}W/m^2/K^4). For LST, the radiative flux footprint is a circular source area of a radius of 250 m (Chow et al. 2014).

We used a set of gridded meteorological forcing products from Livneh et al. (2015, hereafter L15), providing daily precipitation (P), minimum and maximum air temperature ($T_{\min}$ and $T_{\max}$), and wind speed (W_s) at 1/16° (6 km) resolution from 1950 to 2013. L15 is based on the interpolation of weather observations at a number of stations while adjusting for elevation effects. The daily fields of L15 were disaggregated to hourly intervals using the MetSim model (Bohn et al. 2013; Bennett et al. 2020), which was also used to estimate shortwave radiation (R_s), longwave radiation (R_L), and relative humidity. We implemented the triangular method of Bohn et al. (2019) to disaggregate daily precipitation into hourly values using local information on the monthly average storm duration and peak timing. All the meteorological variables were resampled to the size of the VIC grid cell (1 km) using bilinear interpolation.

Remote Sensing Products

To capture land surface conditions, we used a set of time-varying vegetation parameters retrieved from multiple MODIS products, including eight-day composites of Leaf Area Index (LAI; MCD15A2H, 500 m resolution, Myneni et al. 2002) and white-sky shortwave ALB (MCD43A3, 500 m, Schaaf et al. 2002), as well as 16-day composites of Normalized Difference

TABLE 2. Location, elevation, land use-land cover (LULC), and available years for the study period for the AZMET stations and the EC site maintained by Central Arizona–Phoenix Long-Term Ecological Research (CAP-LTER).

Station name	Latitude (°N)	Longitude (°W)	Elevation (m)	LULC	Available years
AZMET					
Buckeye	33.41	−112.68	301	Cropland	2004–2013
Coolidge	32.98	−111.61	423	Cropland	2004–2013
Maricopa	33.07	−111.97	362	Cropland	2004–2013
Paloma	32.93	−112.90	221	Cropland	2004–2013
Queen Creek	33.19	−111.53	462	Cropland	2004–2013
Phoenix Greenway	33.62	−112.11	403	Grass	2004–2013
Phoenix Encanto	33.48	−112.10	334	Grass	2004–2013
Desert Ridge	33.69	−111.96	511	Grass	2004–2013
Mesa	33.39	−111.87	368	Urban	2004–2013
CAP–LTER					
Maryvale	33.48	−112.14	337	Urban	2011–2013

Vegetation Index (NDVI; MOD13A1, 500 m, Huete et al. 2002). We also derived the vegetation fraction (f_v) as $f_v = [(\mathrm{NDVI} - \mathrm{NDVI}_{min})/(\mathrm{NDVI}_{max} - \mathrm{NDVI}_{min})]^2$, where $\mathrm{NDVI}_{min} = 0.1$ and $\mathrm{NDVI}_{max} = 0.8$. Quality control, gap-filling, and interpolation procedures for obtaining f_v are described in Bohn and Vivoni (2019). For urban pixels where LAI estimates are not available from MODIS, we used the LAI product retrieved from the Satellite Pour l'Observation de la Terre (SPOT) satellite system (10 days, 1 km) provided by Copernicus Global Land Service (CGLS; http://land.copernicus.eu/global/products). While these products are fairly coarse for the characterization of urban and agricultural areas, these are consistent with the resolution adopted in VIC and the available LST products used for model evaluation.

To illustrate the remote sensing products over the study region, Figures 2 and 3 present the spatiotemporal variations in P and f_v. Note that the spatial variability of mean annual P is controlled by elevation, as shown by Mascaro (2017), while its interannual variability is largely due to marked differences in winter and summer seasons, consistent with Sheppard et al. (2002). In general, natural ecosystems tend to have a lower f_v than agricultural and urban areas that receive irrigation. Nevertheless, natural ecosystems, such as shrublands, exhibit a high sensitivity to P such that vegetation adapts in greenness to intraannual and interannual variability in precipitation (Forzieri et al. 2011; Vivoni 2012). Cropland and urban areas, in contrast, contain large values of f_v and are generally less susceptible to precipitation variations, but show the signature of the irrigation practices and cropping patterns (Zheng et al. 2015). Meanwhile, urban areas have a lower interannual and intraannual variation in f_v as compared to croplands, which is expected as most of the urban vegetation is kept the same across different years and irrigated regularly. This finding is consistent with the Jenerette et al. (2011) who also found a decreasing variability of NDVI in central Arizona from 1970 to 2000 as urban areas expanded. In addition, urban areas and cropland have different spatial patterns that persist into the 1-km resolution of the VIC model. For example, urban areas are generally concentrated near the center of the region, whereas crop areas are more scattered around the periphery. This pattern corresponds to the historical expansion of small towns in the region into the surrounding agricultural landscape (Hirt et al. 2008). In addition, urban areas tend to have a larger number of smaller patches as a consequence of continuous urbanization. In comparison, the cropland areas have a lower degree of fragmentation (Luck and Wu 2002).

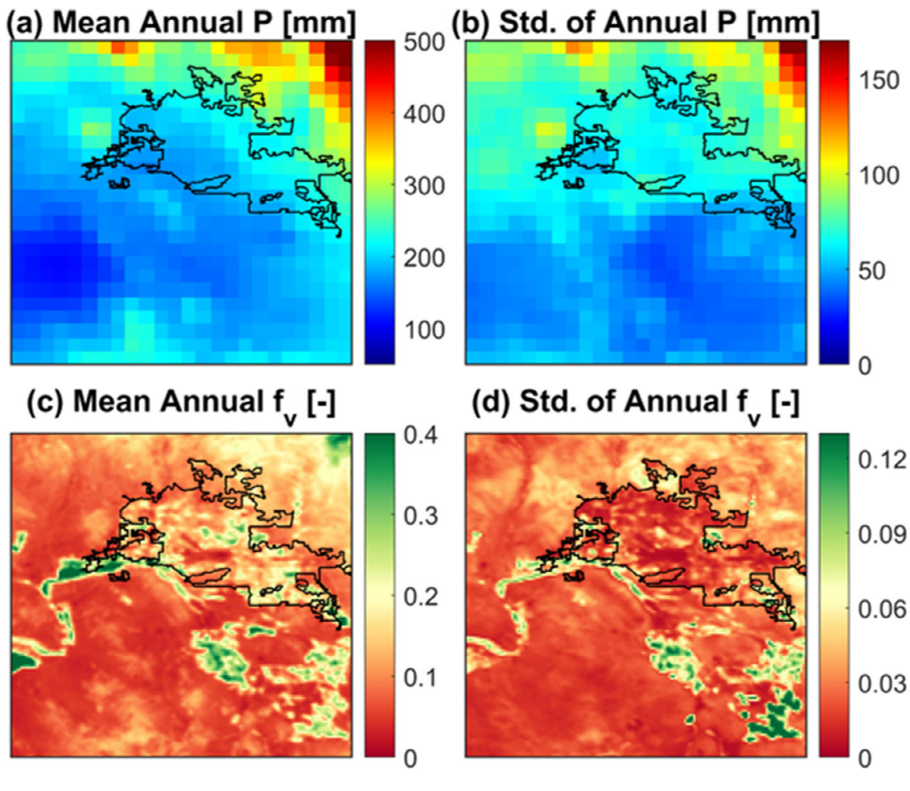

FIGURE 2. Spatial distribution of (a) mean annual precipitation (P), (b) standard deviation (std) of annual P, (c) mean annual vegetation fraction (f_v), and (d) std of f_v (2004–2013).

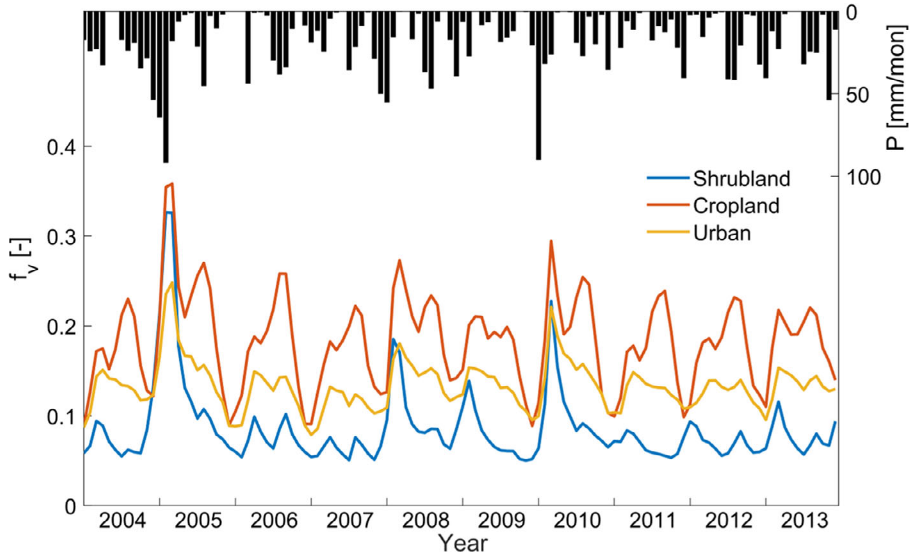

FIGURE 3. Mean monthly P and f_v over shrubland, cropland, and urban area during 2004–2013.

Two remotely sensed LST products with different spatial and temporal resolutions were used for model validation. First, daily LST products (MYD11A1 and MOD11A1, 1 km, Version 6) from MODIS satellites (Aqua and Terra) were obtained (Wan et al. 2004). MODIS satellites overpass the equator twice per day, with daytime overpass times around 1100 and 1300 and nighttime overpass times around 2200 and 0200 for Terra and Aqua (local time). MODIS LST products were obtained from the NASA Earthdata server and processed with the "MODIStsp" R package (Busetto and Ranghetti 2016). Imageries with >10% of missing data (mostly due to cloud presence) were discarded for quality control purposes (Hu et al. 2014). We also obtained the hourly LST product (5 km) retrieved from GOES satellites (Yu et al. 2009) from CGLS (available since October 2010) over the years 2011 to 2013. Table 3 provides a summary of all datasets used in this study, including variable names, data sources, resolutions, and usage.

TABLE 3. Summary of the datasets used in the study including ground observations, gridded meteorological datasets, and remotely sensed products. The variables include precipitation (P), daily maximum air temperature (T_{max}), daily minimum air temperature (T_{min}), wind speed (W_s), Leaf Area Index (LAI), Normalized Difference Vegetation Index (NDVI), albedo (ALB), canopy fraction (f_v), irrigation fraction (f_{irr}), and land surface temperature (LST).

Variables	Source and resolutions	Usage
Ground observations		
P, T_{max}, T_{min}, W_s	AZMET, one hour, point	Bias correction
ET, R_L	CAP-LTER, 30 min, point	Model evaluation
Gridded meteorological datasets		
P, T_{max}, T_{min}, W_s	L15, 6 km, daily	Meteorological forcings
Remote sensing products		
LAI, ALB, NDVI, f_v	MODIS, 500 m, 16 day	Vegetation parameters
Land cover classes	NLCD, three year, 30 m	Vegetation parameters
Land cover classes	NLUD, 10 year, 90 m	Vegetation parameters
Crop f_{irr}	CDL, one year, 30 m	Irrigation fraction
Urban f_{irr}	NAIP, one year, 1 m	Irrigation fraction
LST	MODIS, 12 h, 1 km	Model evaluation
LST	GOES, one hour, 5 km	Model evaluation

Notes: MODIS, Moderate Resolution Imaging Spectroradiometer; CDL, Cropland Data Layer; NAIP, National Agricultural Imagery Program; GOES, Geostationary Operational Environmental Satellite.

METHODOLOGY

Model Overview and Setup

The VIC model version 5.1 (Hamman et al. 2018) was used to simulate land surface water and energy storages and fluxes. We ran VIC at 1 km resolution and an hourly time step over the period 2004 to 2013, with three years of model spin-up (2001–2003). Within each grid cell, VIC represents the surface as a mosaic of tiles each containing a homogeneous vegetation (or land use) class atop a three-layer soil column. We utilized the energy balance mode of the VIC model to evaluate the influence of irrigation on LST.

This mode iteratively solves for LST to minimize the error obtained in the surface energy balance closure at each timestep. It requires more computational effort as the surface energy fluxes depending on surface temperature (sensible heat, latent heat, and ground heat) are calculated simultaneously in each iteration to compensate for the net radiation (more details in Liang et al. 1994). For this study, we used a version of VIC that has been improved in its representation of ET in arid and semiarid regions (Bohn and Vivoni 2016; Bohn et al. 2018). The model improvements include: (1) a new clumped vegetation scheme that divides each vegetation tile into vegetated and nonvegetated areas (i.e., bare soil), which is more appropriate for the sparse vegetation in the study region; (2) parameterizing the vegetation fraction (f_v) as well as other parameters (LAI, ALB) with remotely sensed observations; and (3) a sprinkler-type irrigation scheme with a monthly variation of irrigation fractions (f_{irr}), which is important to represent cropping practices and changes in cropland areas (Fan et al. 2014; Shi et al. 2018). In each timestep, water is applied to the irrigated portion of each grid cell as a supplement to P in order to avoid water stress in crops or urban plants. Similar irrigation schemes have been widely used in LSMs (Ozdogan et al. 2010; Leng et al. 2013) and energy balance models (Dhungel et al. 2019). Soil moisture deficit irrigation starts when the top layer soil moisture (θ) drops below the critical point and continues until θ reaches saturation. Using this approach, VIC has been previously used to evaluate the influence of irrigation (e.g., Bohn et al. 2018; Chen et al. 2018; Shah et al. 2019).

Irrigation Fraction and Soil Map

To determine urban and agricultural irrigation fractions (Figure 4a), we merged two high-resolution land cover maps. For urban irrigation, we used a high-resolution land cover map (1 m) from the National Agricultural Imagery Program in the year 2010. As described in Li, Myint, et al. (2014), this map classifies the PMA into roads, buildings, soil or rock, vegetation, cultivated land, and open water bodies. Given the need for urban irrigation to support vegetation in Phoenix, we assumed that pixels classified as tree and grass were irrigated. We then derived the irrigation fraction for all urban land use types using spatial aggregation by grouping the 1 m vegetation into the 30 m NLCD classes occurring with each 1 km grid cell. For crop irrigation, we used the Cropland Data Layer product, which provides crop

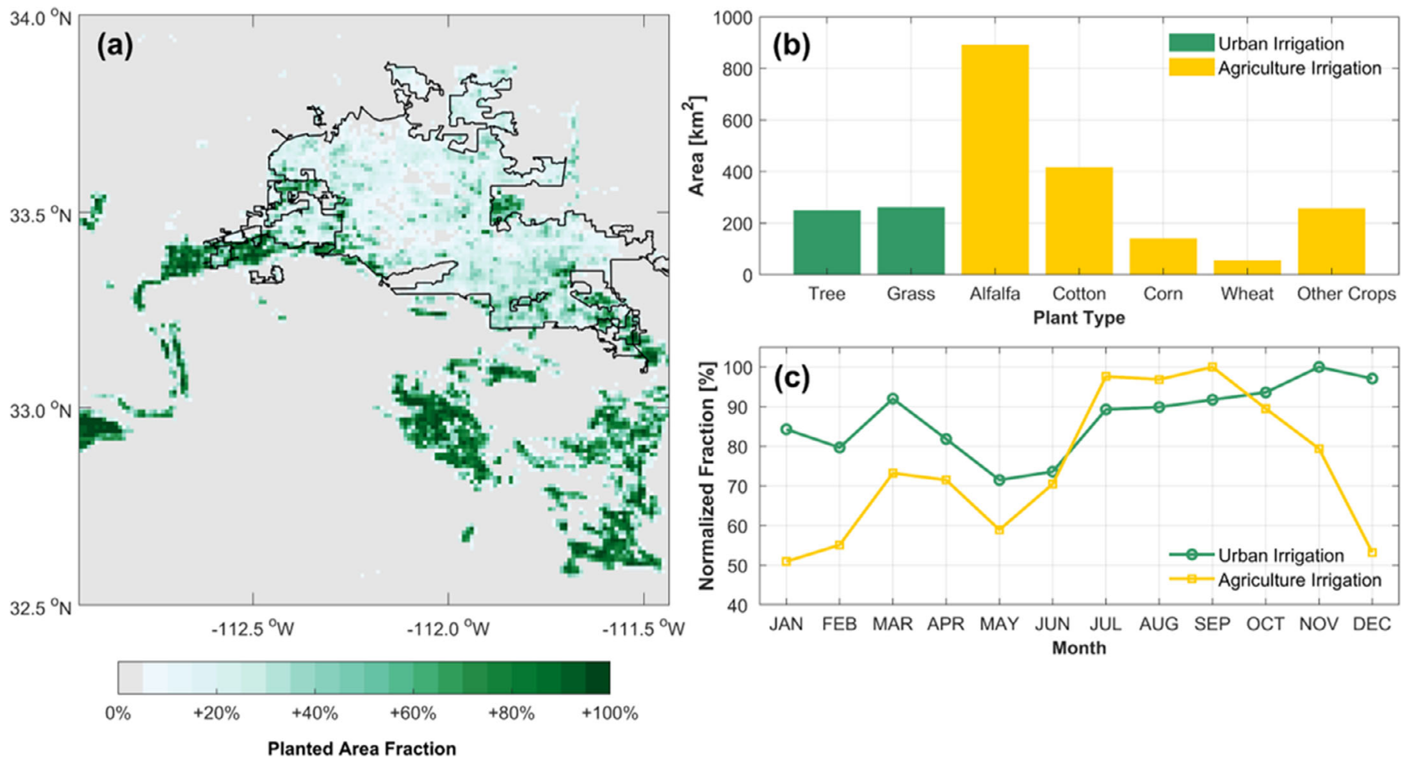

FIGURE 4. (a) Planted area fraction, (b) total area of irrigation by plant type, and (c) monthly irrigation fraction for urban and agricultural areas.

type information at 30 m resolution (Wickham et al. 2014). Resulting from this analysis, we found that the total irrigated area is 570.02 km^2 (43.67% tree, 45.84% grass, and 10.49% shrub) in urban regions and 1,723.34 km^2 in croplands, among which alfalfa (47.55%) and cotton (30.15%) are dominant classes (Figure 4b). To determine the irrigation duration, we used NDVI as a phenological indicator given its prior use in central Arizona (Zheng et al. 2015). We used a threshold detection method to determine the irrigation period, resulting in an irrigation scheme that is turned on when NDVI is higher than the selected threshold (0.23 and 0.25 for urban and cropland areas). Monthly irrigation fractions for urban and agricultural lands over the study period are shown in Figure 4c.

Recent VIC modeling studies typically use soil properties from L15 obtained from the FAO-UNESCO Digital Soil Map of the World and calibrated in previous studies (Maurer et al. 2002; Livneh et al. 2013). However, the spatial resolution (12 km) is too coarse to be compatible with the high-resolution vegetation datasets used in this study. To address this, we conducted a high-resolution mapping of soil type from the clay, silt, and sand fractions obtained from the SoilGrids250m product (Hengl et al. 2017) based on the United States (U.S.) Department of Agriculture soil classification scheme. Once the soil type was determined, the soil properties were obtained from the library of VIC soil parameters (available at http://vic.readthedocs.io/en/master/Documentation/soiltext) for the three soil layers specified in the model. For the irrigation simulation, the key soil parameters include the thickness of the top soil layer, bulk density, soil density, fractional soil moisture content at the critical point, and saturated hydraulic conductivity.

Numerical Experiments and Model Evaluation

We first conducted two sets of VIC experiments with the irrigation scheme turned off (VIC-NOIRR) and on (VIC-IRR) as shown in Table 4. Model comparisons of ET were carried out with the EC datasets in year 2012. We then compared simulated LST with GOES from 2011 to 2013 and MODIS from 2004 to 2013, based on forcing data availability. After the model evaluation, we explored the spatiotemporal variation of ICC by conducting a set of experiments using dynamic (DYN) and climatological (CLM) vegetation parameters with irrigation turned on or off. Vegetation parameters and irrigation fractions used in CLM were calculated as average monthly values from 2004 to 2013. In contrast, the DYN experiment allows for interannual variations responding to climate variations and differences in agricultural management. The ICC metric, which is similar to the urban water capacity proposed by W19, is defined as the amount of irrigation water needed to reduce the LST by 1°C, as:

TABLE 4. Numerical experiments. DYN refers to dynamic irrigation fractions and vegetation, whereas CLM refers to static irrigation fractions and climatological vegetation. In both cases, irrigation can be turned on (IRR) and off (NOIRR, 0 irrigation fraction).

Experiment	Irrigation fraction	Vegetation parameters
CLM-NOIRR	0	Climatological
CLM-IRR	Static	Climatological
DYN-NOIRR	0	Dynamic
DYN-IRR	Dynamic	Dynamic

$$\mathrm{ICC} = \frac{\mathrm{Irr}}{\Delta \mathrm{LST}} = \frac{\mathrm{Irr}}{\mathrm{LST_{NOIRR}} - \mathrm{LST_{IRR}}}, \tag{2}$$

where Irr is the daily average irrigation depth (mm/day), calculated as the volumetric water use over the entire grid cell (including both irrigated and nonirrigated tiles), at 1 km resolution, and ΔLST is the difference in LST between the VIC-NOIRR and VIC-IRR cases.

RESULTS

Model Evaluations at EC Tower

We first evaluate the model performance at the EC tower by comparisons of observations to the simulations with the irrigation scheme turned on (VIC-IRR) and off (VIC-NOIRR). Figure 5 compares daily ET over the year 2012 from observations and the VIC simulations at the co-located grid cell (1 km). When the irrigation scheme is turned off, VIC only captures the response of ET to rainfall pulses and significantly underestimated ET during most of the year (correlation coefficient, CC, of 0.25 and root mean square error, RMSE, of 1.60 mm/day). These errors are expected due to outdoor water use in small grass and tree areas around the EC tower (Chow et al. 2014). In contrast, the VIC-IRR simulation captures the seasonal evolution of ET and shows improved performance (CC = 0.73, RMSE = 0.59 mm/day) through the addition of irrigation water (Irr = 2.6 mm/day), consistent with previous efforts of Bohn and Vivoni (2016). For VIC-IRR, there is a very low sensitivity to rainfall forcing errors from the gridded product of

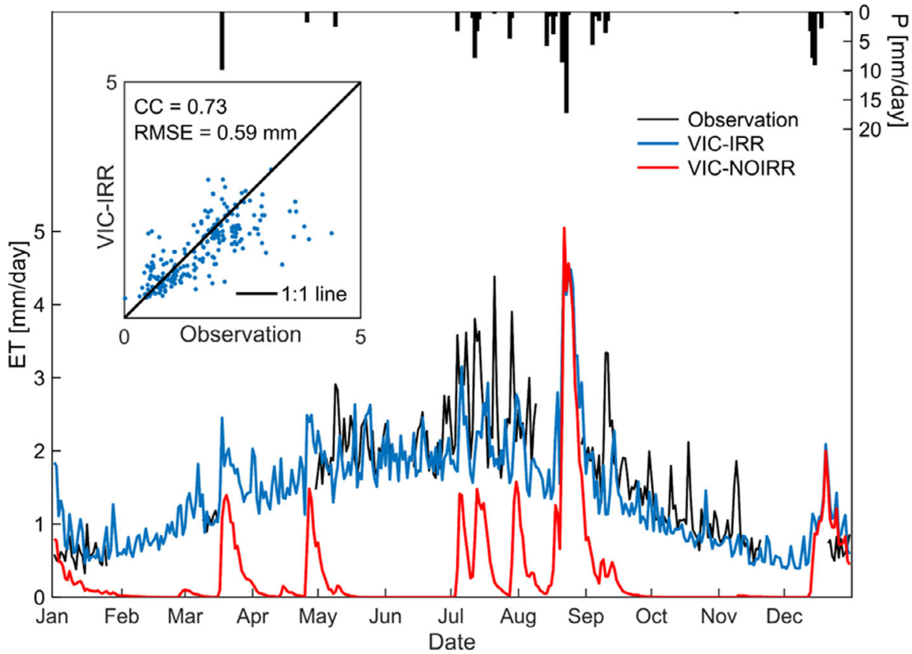

FIGURE 5. Comparison of daily ET from EC observations with the simulations for VIC-NOIRR and VIC-IRR simulations in the year 2012. Inset is a scatter plot of ET (mm/day, n = 222). VIC-IRR, Variable Infiltration Capacity experiments with the irrigation scheme turned on; VIC-NOIRR, Variable Infiltration Capacity experiments with the irrigation scheme turned off.

L15 due to the dominant role of irrigation water input. We note that VIC-IRR and VIC-NOIRR have similar daily ET in August (4.9 and 5.2 mm, respectively) when storm events increase θ, leading to a more limited role of urban irrigation (Templeton et al. 2018).

In Figure 6, we compare LST derived from longwave radiation observations with estimates from MODIS, GOES, and the VIC-IRR simulation. Comparisons are presented as monthly LST differences (MODIS, GOES, or VIC-IRR minus observations) and shown as averages (symbols) and ±1 standard deviation (std) within each month (error bars). Average differences are within $\pm2.0°C$ for GOES during both daytime and nighttime, whereas MODIS has higher discrepancies (up to $\pm5.0°C$). A strong seasonal cycle can be noted in MODIS during the daytime, with the largest positive differences in summer, consistent with prior efforts (Li, Yu, et al. 2014; Beale et al. 2019; Martin et al. 2019). Overall, GOES shows better agreement with LST at the EC tower as compared to MODIS especially during the summer, which may seem counterintuitive considering the higher spatial resolution of MODIS. We attribute this to the consistency in diurnal temporal sampling between GOES and the local observations. Beale et al. (2019) found a similar pattern, finding that the seasonal variance between LST products was due to solar radiation and the time-varying viewing angle. Other sources of satellite LST uncertainty include the retrieval algorithm, atmospheric correction, and surface emissivity (Li et al. 2013). Importantly, the VIC-IRR simulation reproduces daytime and nighttime LST well as compared to observations (+2.75°C and −4.00°C), typically better than MODIS and on occasions comparable to GOES. This suggests VIC-IRR captures LST with an accuracy similar to remote sensing products by resolving the diurnal cycle, with differences due to the spatial variations between the radiometer footprint (~250 m in radius), the size of the VIC grid cell (1 km), and the resolution of the remote sensing products (1 km for MODIS and 5 km for GOES).

Model Evaluations at Regional Scale

We next compared the diurnal cycle of simulated LST with those obtained from GOES averaged over natural shrublands, croplands, and urban areas in the region (Figure 7). As expected from the analysis at the EC tower, VIC has differences with GOES over all the land cover types, but in general, captures the diurnal evolution of LST well. Comparisons over shrub areas with VIC-NOIRR are consistent with previous studies using VIC (Mitchell et al. 2004; Koch et al. 2016). Interestingly, differences between VIC-IRR and GOES are lower in irrigated areas,

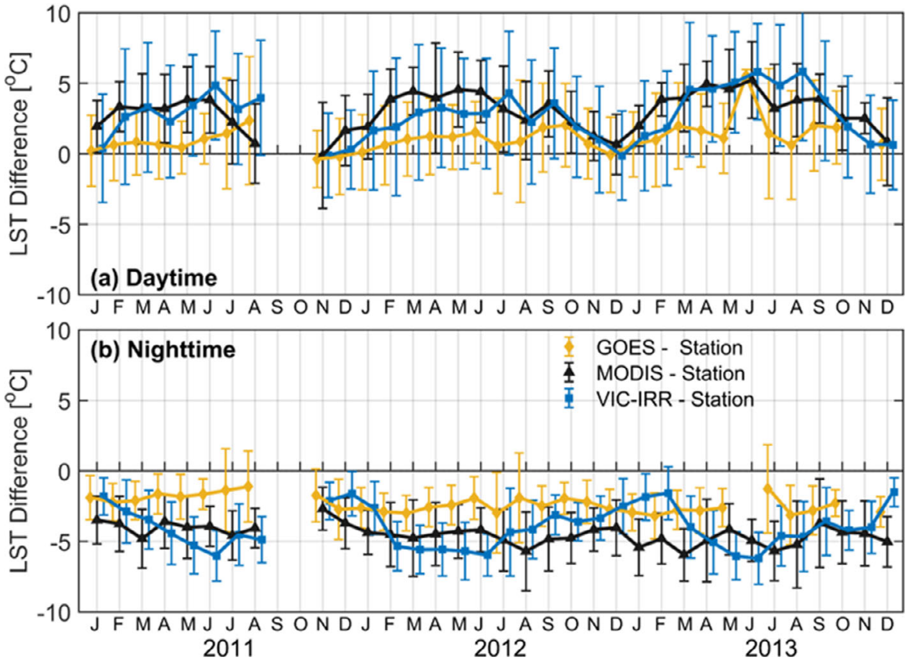

FIGURE 6. Monthly differences (estimate minus observation) at EC tower during (a) daytime and (b) nighttime. Symbols are average values and error bars are ±1 std.

indicating an improvement in the simulations due to the irrigation scheme. Average daily LST differences were reduced for the daytime (0800 to 1700 local time) from 3.2°C to 0.3°C over croplands and from 4.2°C to 1.4°C over urban areas. Furthermore, this shows that VIC-IRR can capture the evaporative cooling effect of irrigation in a means consistent with prior observations (Templeton et al. 2018) and modeling work (Yang et al. 2019). The evaporative cooling effect is also compared to the diurnal cycle of air temperature (T_{air}) obtained from the forcing product for each land cover type. As expected, during most of the daytime (0700–1700 local time), T_{air} is lower than LST, while during the nighttime, T_{air} is larger than LST. Differences in the temporal lags between T_{air} and LST are likely due to the variable heating between the atmosphere and the specific thermal and irrigation conditions in each land cover type (Song et al. 2017). Inspection of particular days (not shown) indicates that the evaporative cooling effect in VIC-IRR can be substantial enough to lead to T_{air} and LST having similar diurnal cycles over the study region, as noted in the work of Vivoni et al. (2020).

Figure 8 presents the spatial patterns of daytime and nighttime LST as obtained from VIC-IRR and MODIS, each averaged over 2004 to 2013. To complement this, Table 5 shows differences (VIC-IRR minus MODIS) and RMSE values for each year. The performance of VIC-IRR is stable across the study period, suggesting that the model can capture LST under different conditions. Due to the cooling effect of irrigation, croplands and urban areas generally exhibit a lower daytime LST as compared with shrublands with no irrigation (39°C and 40°C vs. 41°C), as obtained from MODIS. VIC-IRR captures this pattern well, but exhibits higher daily averaged LST than MODIS over shrublands and urban areas in the daytime (+2.67°C and +2.01°C) and higher LST over croplands at nighttime (+2.34°C). In light of the many factors affecting the simulation of LST, these small differences suggest that the VIC model is reliable for studying the ICC in the region.

Overall, the variations in LST are represented well in the study region and comparable with results from previous modeling efforts (e.g., Xiang et al. 2014; Salamanca et al. 2018; Ko et al. 2019). The model comparison to LST derived from longwave radiation observations showed that the bias of simulated average daily LST is −0.6°C, which is similar to the remote sensing products (−0.6°C and −0.7°C for GOES and MODIS, respectively). At the regional scale, the VIC-IRR simulated LST is 1.1°C lower than MODIS observations when averaged from 2004 to 2013, with RMSE of 4.4°C. The relatively large RMSE values reflected the interplay of uncertainties associated with the meteorological forcing product (L15), vegetation parameterization, and model assumptions made when calculating LST. Nevertheless, the stable model performance of LST across different years under varying climate conditions and

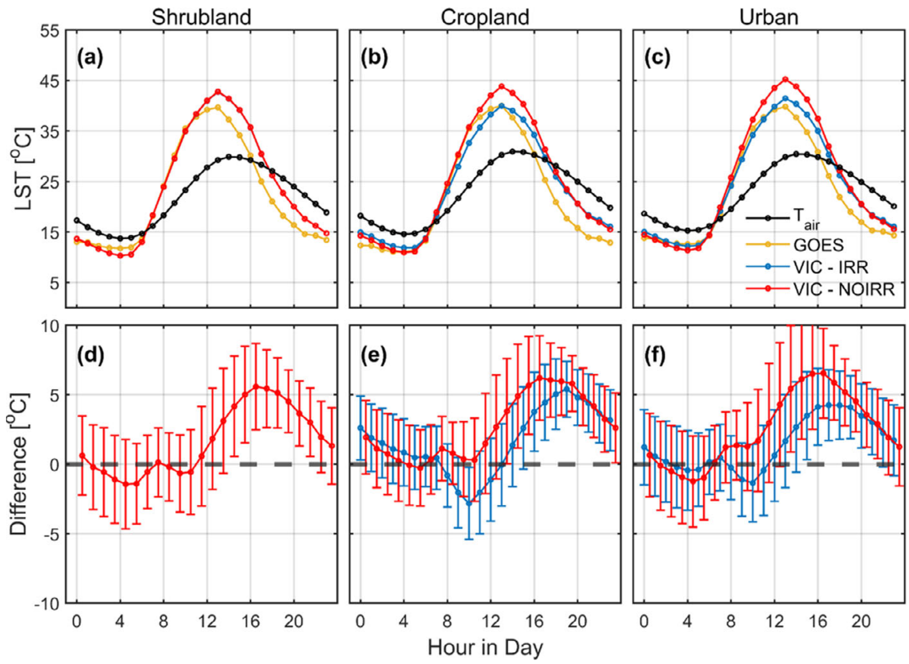

FIGURE 7. Comparison of T_{air} and simulated LST with GOES LST over shrubland, cropland, and urban areas (2011–2013). (a–c) Spatial average T_{air} and LST. (d–f) Average simulation differences (VIC minus GOES) as symbols with ±1 spatial std as error bars.

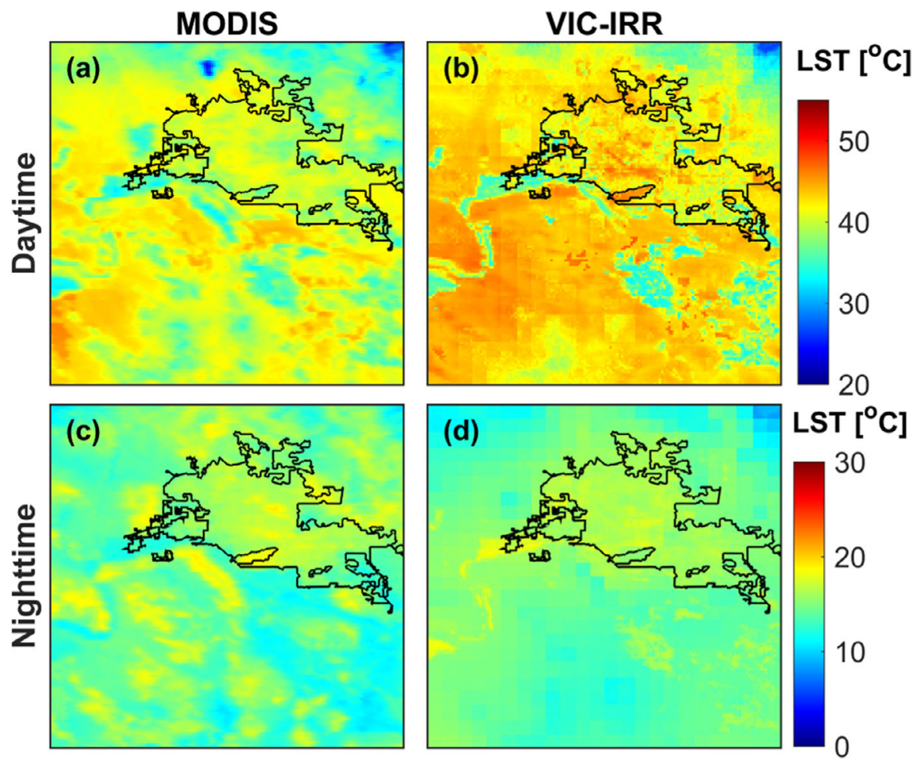

FIGURE 8. Comparison of spatial maps of LST from MODIS and VIC-IRR obtained as averages during daytime and nighttime periods from 2004 to 2013.

TABLE 5. Annual differences (VIC-IRR minus MODIS) and root mean square error (RMSE) in daily average daytime and nighttime LST for shrubland, cropland, and urban areas from 2004 to 2013.

	Difference (RMSE) in °C					
	Daytime			Nighttime		
Year	Shrubland	Cropland	Urban	Shrubland	Cropland	Urban
2004	2.80 (5.37)	0.89 (4.93)	1.91 (4.63)	−0.24 (3.83)	2.79 (4.37)	1.00 (3.25)
2005	2.39 (5.09)	1.22 (4.91)	2.66 (4.85)	−1.51 (4.29)	2.03 (4.07)	0.47 (3.13)
2006	3.09 (5.62)	1.28 (5.11)	2.45 (4.94)	−1.42 (4.21)	2.02 (4.12)	0.06 (3.16)
2007	3.65 (5.89)	1.35 (5.15)	2.58 (4.91)	−0.71 (3.87)	2.22 (4.06)	0.20 (3.05)
2008	2.26 (4.85)	0.87 (4.71)	1.87 (4.39)	−0.41 (4.62)	2.57 (4.87)	0.76 (4.00)
2009	3.11 (5.34)	0.94 (4.95)	2.09 (4.44)	−1.08 (3.91)	2.22 (4.13)	−0.08 (3.10)
2010	2.45 (4.96)	0.83 (4.88)	2.07 (4.59)	−0.87 (3.93)	2.30 (4.12)	0.35 (3.15)
2011	2.88 (5.47)	0.92 (5.11)	1.91 (4.59)	−0.74 (3.84)	2.21 (4.05)	−0.18 (3.11)
2012	1.78 (4.64)	0.18 (4.68)	1.06 (4.04)	−0.51 (3.81)	2.33 (4.10)	−0.23 (3.04)
2013	2.31 (4.94)	0.53 (4.76)	1.59 (4.25)	−0.31 (3.88)	2.75 (4.39)	0.35 (3.17)
All	2.67 (5.23)	0.90 (4.92)	2.01 (4.57)	−0.77 (4.02)	2.34 (4.23)	0.26 (3.22)

irrigation practices indicates that the model is robust in capturing the irrigation cooling effect on LST.

Irrigation Cooling Capacity

Given the confidence obtained on the model performance, we then explored the spatiotemporal variations of the evaporative cooling effect of irrigation. Figure 9 shows the difference between VIC-NOIRR and VIC-IRR ($\Delta LST = LST_{NOIRR} - LST_{IRR}$) averaged over winter (January–March) and summer (July–September) seasons from 2004 to 2013. While irrigation-induced cooling is significant, the magnitude of ΔLST varies for different areas within the study region and for different seasons. For instance, the average ΔLST is higher over croplands (1.85°C) than the urban area (1.43°C) due to a larger f_{irr}. There is also a seasonal evolution of ΔLST, suggesting stronger irrigation cooling effects over croplands and urban areas during the summer (2.49°C and 1.87°C) with more intensive irrigation than in the winter (0.77°C and 0.65°C) which has more limited irrigation. Note that the seasonal average of Irr is 2.32 mm/day in the winter and 4.16 mm/day in the summer for croplands, whereas the average Irr is 1.78 mm/day (winter) and 2.87 mm/day (summer) when averaged over urban areas. In addition, a larger spatial variation of ΔLST is obtained over croplands (std of 1.39°C) as compared to urban areas (std of 0.88°C). This is primarily due to variations in cropping practices in different irrigation districts and at the farm level, including crop rotations, fallow fields, and crop phenology. In contrast, the urban area mostly reflects differences in outdoor water use in vegetated landscaping between low-, medium-, and high-density classes.

We compared the CLM and DYN experiments to determine the effects of interannual variations in climate and vegetation on ICC. CLM only captures year-to-year variations in P, while DYN also includes interannual changes in vegetation parameters (e.g., f_v and f_{irr}). Table 6 summarizes the simulation results with respect to Irr, ΔLST, and ICC for croplands, urban areas, and all irrigated locations. First, we present the relation between annual values of Irr and ΔLST in Figure 10a with the symbol size proportional to annual P (i.e., smaller size is lower P). Irr generally increases as the annual P decreases since additional irrigation is needed to meet the water demand from crops and urban vegetation. The positive relation between Irr and ΔLST implies that higher reductions in LST occur with greater irrigation amounts, as expected. Croplands receive more Irr as compared to urban areas and have larger reductions in LST in both CLM and DYN experiments. As a result, croplands require a higher Irr to obtain a 1°C reduction in LST as captured by ICC in Table 6. Furthermore, the DYN experiment has lower ICC than CLM, implying that time-varying vegetation reduces the need for irrigation for an equivalent reduction of LST. This is consistent with the larger std values obtained in the DYN experiment which includes both climate and vegetation variations from year to year.

To explore this further, we present the spatial variation of the Irr difference between the wettest (2005) and driest (2012) years for the CLM experiment in Figure 10b. Since these years use the same seasonally varying vegetation, any differences are due to meteorological variations, including P and vapor pressure deficit. Differences in Irr are relatively uniform across irrigated areas, with croplands having slightly higher values than urban areas (0.33 vs. 0.22 mm/day). Interannual variations in climate conditions have a modest control on ICC

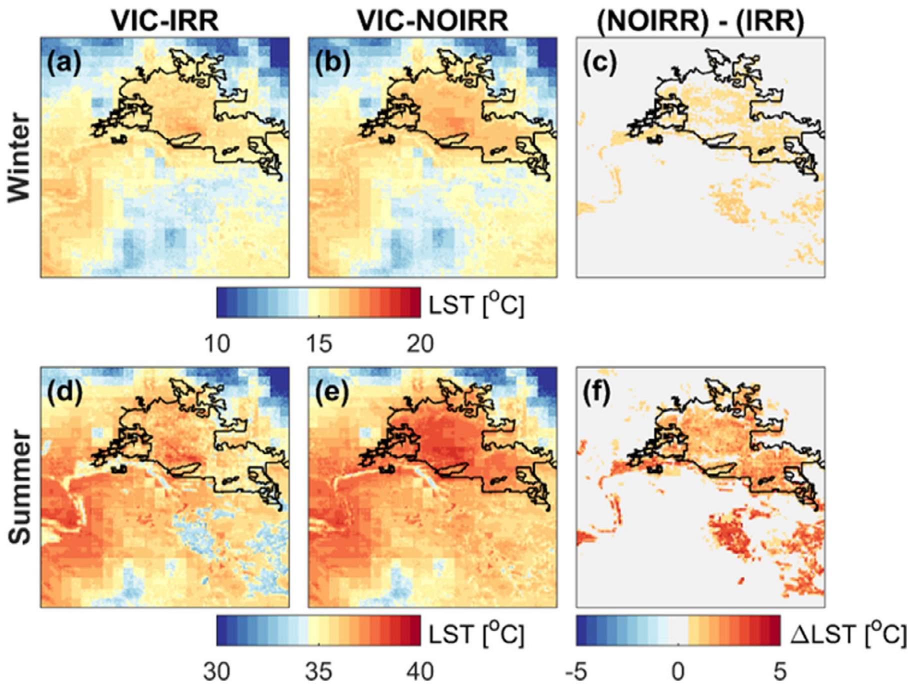

FIGURE 9. Comparison of LST between VIC-IRR and VIC-NOIRR during winter (January–March) and summer (July–September) seasons from 2004 to 2013 and their difference (ΔLST).

TABLE 6. Mean and std of Irr, ΔLST, and ICC for cropland, urban, and all irrigated areas for experiments with CLM and DYN vegetation parameters.

	Mean (std)					
	Irr (mm/day)		ΔLST (°C)		ICC (mm/day/°C)	
Areas	**CLM**	**DYN**	**CLM**	**DYN**	**CLM**	**DYN**
Cropland	3.36 (1.26)	3.31 (1.44)	1.79 (0.48)	1.85 (0.55)	2.06 (0.17)	1.99 (0.21)
Urban	2.29 (0.70)	2.31 (0.73)	1.41 (0.32)	1.43 (0.33)	1.78 (0.14)	1.77 (0.14)
All	2.82 (1.15)	2.80 (1.25)	1.61 (0.45)	1.64 (0.50)	1.91 (0.21)	1.87 (0.20)

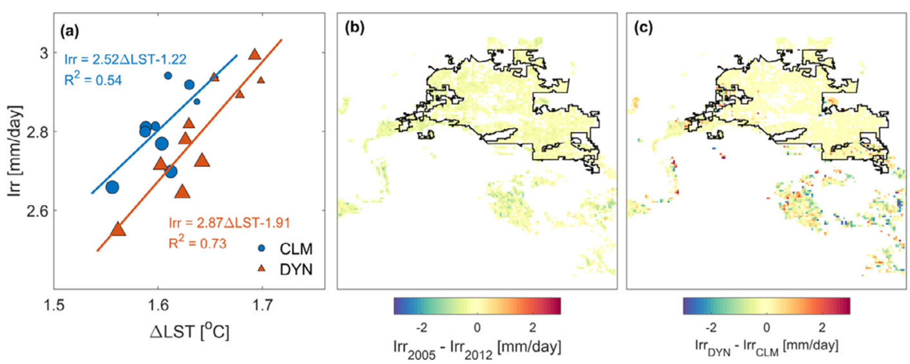

FIGURE 10. (a) Dependence of irrigation amount (Irr) on ΔLST over irrigated areas from 2004 to 2013 for the CLM and DYN experiments. (b) Difference in Irr for CLM between 2005 and 2012. (c) Difference in Irr between DYN and CLM for 2008.

(difference of 0.07 mm/day/°C between 2005 and 2012), especially in urban areas where irrigation is consistent from year to year. In contrast, the impact of dynamic vegetation on Irr and ICC is significant, as demonstrated in the spatial variation of the difference in Irr between the DYN and CLM experiments (Irr_{DYN}–Irr_{CLM}) in Figure 10c for the year 2008 which had an average value of *P*. Clearly, the difference in Irr has large spatial variability, especially over croplands (std of 1.44 mm/day). The magnitude of Irr difference (average of 0.13 mm/day) demonstrates that the dynamic interannual variation of land surface conditions, particularly over agricultural areas with varying cropping practices, has a more important effect than year-to-year differences in climatic conditions. Thus, capturing vegetation parameters in central Arizona from remote sensing products is considered essential for adequately representing the irrigation cooling efficiency.

DISCUSSION

Uncertainty of Remote Sensing Products

While the study results shed light on the value of simulated LST for tracking the effects of irrigation, there are uncertainties associated with the remote sensing products used to build confidence in the model. Due to their relative coarse spatial resolutions, MODIS products generally encounter the mixed pixel problem when compared to higher resolution datasets from other platforms such as Landsat and SPOT (Tian et al. 2002). As compared to irrigated croplands, urban areas have a more heterogeneous structure with both built and natural surfaces, which consequently may increase the classification uncertainty and retrieval algorithms in MODIS Yang et al. (2014). For example, we compared MODIS and Landsat NDVI over a vegetated golf course in Phoenix from 2004 to 2007, finding similar seasonal variations; however, MODIS NDVI is ~8% lower than Landsat NDVI values. As a consequence, the VIC model parameterization can be improved by using remote sensing products with higher spatial resolution and spectral accuracy or through the use of data fusion products, for example, the Spatial and Temporal Reflectance Unmixing Model (STRUM, Gevaert and García-Haro 2015).

Improvements in Modeling Approach

Despite the acceptable model performance in reproducing LST observations, further improvements are possible. In particular, we used a simple NDVI threshold to determine the irrigation period and a soil moisture deficit approach that might deviate from urban and agricultural practices. For example, cotton irrigation in central Arizona begins before plant germination. As a result, the initial watering period is not detectable from NDVI (Thorp et al. 2017). We estimate that this would cause a 10%–20% underestimation of irrigation water use. Given that cotton occupies about 30% of croplands in the region, there is a need to improve the parameterization of the irrigation period for this specific crop. In addition, some urban plants might not have NDVI signal that allows the threshold method to work, especially during winter seasons. This suggests that urban irrigation practices that capture residential landscaping choices (e.g., Volo et al. 2014; Vivoni et al. 2020) should be included in future studies.

Impact of Model Bias on ICC

There are considerable challenges to diagnosing the individual contributions of the various uncertainties in the VIC simulations of LST over the study region. Future studies using structured scenarios that vary individual component processes, along with intercomparison to other models (e.g., Xiang et al. 2017), and the use of innovative spatial performance metrics (e.g., Mascaro et al. 2015; Koch et al. 2016) would be fruitful avenues. The bias of simulated LST across the study domain (+1.86°C and +0.26°C for daytime and nighttime, respectively) corresponds to 4.6% and 4.8% of MODIS LST observations (40°C and 15°C for daytime and nighttime) in relative terms. Model results showed that 2.0 mm/day of irrigation is required to reduce LST by 1°C across the region, with slightly lower values in urban areas (1.8 mm/day). As a result, it is appropriate to consider a model error of 5% when simulating LST changes resulting from applied irrigation. This suggests that the average ICC (2.0 mm/day/°C) might vary from 1.9 to 2.1 mm/day/°C when considering the estimated error in simulating LST.

CONCLUSIONS

As a key state variable of the surface energy and water balance, LST has received attention due to the embedded signature of climate variability superimposed on site-specific properties such as soil, vegetation, and topographic conditions, as well as management activities (Xiang et al. 2014; Ko et al.

2019; Yang et al. 2020). In this study, we utilized the strong effect of irrigation on LST in an arid and semiarid region to test a high-resolution modeling system. Through detailed comparisons to multiyear observations spanning from a single site up to the regional scale, we demonstrated the VIC model capacity using a soil moisture deficit irrigation scheme to reliably reproduce the diurnal cycle, seasonal variations, and spatial differences in LST. The model was further used to evaluate the spatiotemporal variations of ICC over the agricultural–urban interface in central Arizona. Results from the study indicate:

1. Through a series of improvements to the VIC application, the model achieved a good representation of LST as compared to ground and remotely sensed observations over shrubland, cropland, and urban areas. While some mismatches exist between simulations and observations, these are likely due to uncertainties in the gridded forcing and the complex nature of irrigation practices. More importantly, the model reproduced the large reductions in LST due to irrigation. For instance, the average LST over irrigated croplands is 3°C (or 7% in relative terms) lower than surrounding shrublands during the daytime (~43°C) based on VIC simulations.
2. Numerical experiments (VIC-IRR and VIC-NOIRR) revealed the spatiotemporal variations of LST reduction and their underlying controls. Model results also showed that the irrigation cooling effect on LST is more pronounced (by ~1.47°C) during the summer than in the winter. Additionally, a larger LST reduction (by ~0.42°C) occurs in irrigated croplands as compared to urban areas. Larger spatiotemporal variations are noted in LST from year to year in croplands, which is consistent with the identified spatiotemporal variations in the irrigation fraction and land surface properties. This suggests the importance of the irrigation scheme as well as the proper parameterization of irrigation for modeling LST correctly.
3. Through the various experiments, we identified that the interannual variability in cropping practices has a dominant effect on irrigation water use that is considerably stronger than variations in meteorological conditions across different years. In addition, accounting for time-varying vegetation generally reduces the need for irrigation to achieve an equivalent reduction of LST. These findings imply that quantifying how irrigation can ameliorate heat in central Arizona must account for decisions made in irrigation districts and at the individual farm level.

To conclude, the modeling effort resulted in spatiotemporal patterns that represented well the observed differences between urban, cropland, and natural ecosystems lending support to its use for quantifying the irrigation cooling efficiency in central Arizona. Furthermore, this work highlights the essential nature of time-varying vegetation parameters for reliable LSM performance in evaluating irrigation water demand and its evaporative cooling effects. As such, a fruitful avenue of research is to incorporate remotely sensed products to determine the spatiotemporal patterns of vegetation conditions in evaluations of ICC in other regions with outdoor water use. The impacts of these dynamics should also be taken into account when considering the impact of irrigation on atmospheric conditions, for instance, through coupled land-atmosphere modeling (e.g., Xiang et al. 2018; Yang et al. 2019).

ACKNOWLEDGMENTS

This work is supported by NSF (SES–1462086 DCDC III: Transformational Solutions for Urban Water Sustainability Transitions in the Colorado River Basin) and NASA (80NSSC19K1198: Averting Drought Shortages in the Colorado River). Summer support from the UREX Sustainability Research Network and CAP-LTER for Zhaocheng Wang is also acknowledged. The authors thank the contributions of the following individuals during various stages of this effort: Chenghao Wang, Eli R. Perez-Ruiz, Giuseppe Mascaro, and Kristen M. Whitney. The authors also acknowledge the computing facilities at the ASU Advanced Computing Center. The source code of VIC can be found at GitHub (http://www.github.com/tbohn/VIC/releases/tag/v1). The flux tower datasets and land cover map can be obtained from the CAP-LTER Data Catalog (http://sustainability.asu.edu/caplter/data/). The NLUD product can be downloaded from the U.S. Environmental Protection Agency (https://www.epa.gov/iclus/iclus-data-southwest-region).

AUTHORS' CONTRIBUTIONS

Zhaocheng Wang: Conceptualization; data curation; formal analysis; investigation; methodology; resources; software; validation; visualization; writing-original draft; writing-review & editing. **Enrique R. Vivoni:** Conceptualization; funding acquisition; project administration; resources; supervision; writing-review & editing. **Theodore J. Bohn:** Data curation; methodology; software; writing-review & editing. **Zhi-Hua Wang:** Methodology; resources; writing-review & editing.

LITERATURE CITED

Balling, R.C., P. Gober, and N. Jones. 2008. "Sensitivity of Residential Water Consumption to Variations in Climate: An Intraurban Analysis of Phoenix, Arizona." *Water Resources Research* 44 (10). https://doi.org/10.1029/2007WR006722.

Beale, C., H. Norouzi, Z. Sharifnezhadazizi, A.R. Bah, P. Yu, Y. Yu, R. Blake, A. Vaculik, and J. Gonzalez-Cruz. 2019. "Comparison of Diurnal Variation of Land Surface Temperature From GOES-16 ABI and MODIS Instruments." *IEEE Geoscience and Remote Sensing Letters* 17 (4): 572–76. https://doi.org/10.1109/LGRS.2019.2930174.

Bennett, A.R., J.J. Hamman, B. Nijssen, and S. Pfenninger. 2020. "MetSim: A Python Package for Estimation and Disaggregation of Meteorological Data." *Journal of Open Source Software* 5 (47): 2042. https://doi.org/10.21105/joss.02042.

Bohn, T.J., B. Livneh, J.W. Oyler, S.W. Running, B. Nijssen, and D.P. Lettenmaier. 2013. "Global Evaluation of MTCLIM and Related Algorithms for Forcing of Ecological and Hydrological Models." *Agricultural and Forest Meteorology* 176: 38–49. https://doi.org/10.1016/j.agrformet.2013.03.003.

Bohn, T.J., and E.R. Vivoni. 2016. "Process-Based Characterization of Evapotranspiration Sources over the North American Monsoon Region." *Water Resources Research* 52 (1): 358–84. https://doi.org/10.1002/2015WR017934.

Bohn, T.J., and E.R. Vivoni. 2019. "MOD-LSP, MODIS-Based Parameters for Hydrologic Modeling of North American Land Cover Change." *Scientific Data* 6: 144. https://doi.org/10.1038/s41597-019-0150-2.

Bohn, T.J., E.R. Vivoni, G. Mascaro, and D.D. White. 2018. "Land and Water Use Changes in the US–Mexico Border Region, 1992–2011." *Environmental Research Letters* 13 (11): 1992–2011. https://doi.org/10.1088/1748-9326/aae53e

Bohn, T.J., K.M. Whitney, G. Mascaro, and E.R. Vivoni. 2019. "A Deterministic Approach for Approximating the Diurnal Cycle of Precipitation for Use in Large-scale Hydrological Modeling." *Journal of Hydrometeorology* 20 (2): 297–317. https://doi.org/10.1175/JHM-D-18-0203.1.

Busetto, L., and L. Ranghetti. 2016. "MODIStsp: An R Package for Automatic Preprocessing of MODIS Land Products Time Series." *Computers and Geosciences* 97: 40–48. https://doi.org/10.1016/j.cageo.2016.08.020.

Chen, Y., J. Niu, S. Kang, and X. Zhang. 2018. "Effects of Irrigation on Water and Energy Balances in the Heihe River Basin Using VIC Model under Different Irrigation Scenarios." *Science of The Total Environment* 645: 1183–93. https://doi.org/10.1016/J.SCITOTENV.2018.07.254.

Chow, W.T.L., D. Brennan, and A.J. Brazel. 2012. "Urban Heat Island Research in Phoenix, Arizona." *Bulletin of the American Meteorological Society* 93 (4): 517–30. https://doi.org/10.1175/BAMS-D-11-00011.1.

Chow, W.T.L., T.J. Volo, E.R. Vivoni, G.D. Jenerette, and B.L. Ruddell. 2014. "Seasonal Dynamics of a Suburban Energy Balance in Phoenix, Arizona." *International Journal of Climatology* 34 (15): 3863–80. https://doi.org/10.1002/joc.3947.

Dhungel, R., R. Aiken, P.D. Colaizzi, X. Lin, D. O'Brien, R.L. Baumhardt, D.K. Brauer, and G.W. Marek. 2019. "Evaluation of Uncalibrated Energy Balance Model (BAITSSS) for Estimating Evapotranspiration in a Semiarid, Advective Climate." *Hydrological Processes* 33 (15): 2110–30. https://doi.org/10.1002/hyp.13458.

Fan, C., B. Zheng, S.W. Myint, and R. Aggarwal. 2014. "Characterizing Changes in Cropping Patterns Using Sequential Landsat Imagery: An Adaptive Threshold Approach and Application to Phoenix, Arizona." *International Journal of Remote Sensing* 35 (20): 7263–78. https://doi.org/10.1080/01431161.2014.967891.

Forzieri, G., F. Castelli, and E.R. Vivoni. 2011. "Vegetation Dynamics within the North American Monsoon Region." *Journal of Climate* 24 (6): 1763–83. https://doi.org/10.1175/2010JCLI3847.1.

Georgescu, M., G. Miguez-Macho, L.T. Steyaert, and C.P. Weaver. 2008. "Sensitivity of Summer Climate to Anthropogenic Land-Cover Change over the Greater Phoenix, AZ, Region." *Journal of Arid Environments* 72 (7): 1358–73. https://doi.org/10.1016/j.jaridenv.2008.01.004.

Gevaert, C.M., and F.J. García-Haro. 2015. "A Comparison of STARFM and an Unmixing-Based Algorithm for Landsat and MODIS Data Fusion." *Remote sensing of Environment* 156: 34–44. https://doi.org/10.1016/j.rse.2014.09.012.

Gober, P. 2006. *Metropolitan Phoenix: Place making and community building in the desert*. University of Pennsylvania Press. https://doi.org/10.9783/9780812205824.169.

Gober, P., and C.W. Kirkwood. 2010. "Vulnerability Assessment of Climate-Induced Water Shortage in Phoenix." *Proceedings of the National Academy of Sciences of the United States of America* 107 (50): 21295–99. https://doi.org/10.1073/pnas.0911113107

Gober, P., A. Middel, A. Brazel, S. Myint, H. Chang, J.D. Duh, and L. House-Peters. 2012. "Tradeoffs between Water Conservation and Temperature Amelioration in Phoenix and Portland: Implications for Urban Sustainability." *Urban Geography* 33 (7): 1030–54. https://doi.org/10.2747/0272-3638.33.7.1030.

Hamman, J.J., B. Nijssen, T.J. Bohn, D.R. Gergel, and Y. Mao. 2018. "The Variable Infiltration Capacity Model Version 5 (VIC-5): Infrastructure Improvements for New Applications and Reproducibility." *Geoscientific Model Development* 11 (8). https://doi.org/10.5194/gmd-11-3481-2018.

Hengl, T., J. Mendes de Jesus, G.B.M. Heuvelink, M. Ruiperez Gonzalez, M. Kilibarda, A. Blagotić, W. Shangguan *et al*. 2017. "SoilGrids250m: Global Gridded Soil Information Based on Machine Learning." *PLoS One* 12 (2): e0169748. https://doi.org/10.1371/journal.pone.0169748.

Higdon, P.H., and T.W. Thompson. 1980. "The 1980 Arizona Groundwater Management Code." *Arizona State Law Journal* 1980 (3): 621–72.

Hirt, P., A. Gustafson, and K. Larson. 2008. "The Mirage in the Valley of the Sun." *Environmental History* 13 (3): 482–514. https://doi.org/10.1093/envhis/13.3.482.

Homer, C., J. Dewitz, L. Yang, S. Jin, P. Danielson, G. Xian, J. Coulston, N. Herold, J. Wickham, and K. Megown. 2015. "Completion of the 2011 National Land Cover Database for the Conterminous United States–Representing a Decade of Land Cover Change Information." *Photogrammetric Engineering & Remote Sensing* 81 (5): 345–54. https://pubs.er.usgs.gov/publication/70146301.

Hu, L., N.A. Brunsell, A.J. Monaghan, M. Barlage, and O.V. Wilhelmi. 2014. "How Can We Use MODIS Land Surface Temperature to Validate Long-Term Urban Model Simulations?" *Journal of Geophysical Research: Atmospheres* 119 (6): 3185–201. https://doi.org/10.1002/2013JD021101.

Huete, A., K. Didan, T. Miura, E.P. Rodriguez, X. Gao, and L.G. Ferreira. 2002. "Overview of the Radiometric and Biophysical Performance of the MODIS Vegetation Indices." *Remote sensing of environment* 83 (1–2): 195–213. https://doi.org/10.1016/S0034-4257(02)00096-2.

Jenerette, G.D., S.L. Harlan, W.L. Stefanov, and C.A. Martin. 2011. "Ecosystem Services and Urban Heat Riskscape Moderation: Water, Green Spaces, and Social Inequality in Phoenix, USA." *Ecological Applications* 21 (7): 2637–51. https://doi.org/10.1890/10-1493.1.

Kerna, A., and G. Frisvold. 2014. *Agriculture in Arizona's Economy: An Economic Contribution Analysis*. Tucson, AZ: Department of Agricultural & Resource Economics, University of Arizona.

Ko, A., G. Mascaro, and E.R. Vivoni. 2016. "Irrigation Impacts on Scaling Properties of Soil Moisture and the Calibration of a

Multifractal Downscaling Model." *IEEE Transactions on Geoscience and Remote Sensing* 54 (6): 3128–42. https://doi.org/10.1109/TGRS.2015.2511628.

Ko, A., G. Mascaro, and E.R. Vivoni. 2019. "Strategies to Improve and Evaluate Physics-Based Hyperresolution Hydrologic Simulations at Regional Basin Scales." *Water Resources Research* 55 (2): 1129–52. https://doi.org/10.1029/2018WR023521.

Koch, J., A. Siemann, S. Stisen, and J. Sheffield. 2016. "Spatial Validation of Large-Scale Land Surface Models Against Monthly Land Surface Temperature Patterns Using Innovative Performance Metrics." *Journal of Geophysical Research: Atmospheres* 121 (10): 5430–52. https://doi.org/10.1002/2015JD024482.

Leng, G., M. Huang, Q. Tang, W.J. Sacks, H. Lei, and L.R. Leung. 2013. "Modeling the Effects of Irrigation on Land Surface Fluxes and States over the Conterminous United States: Sensitivity to Input Data and Model Parameters." *Journal of Geophysical Research Atmospheres* 118 (17): 9789–803. https://doi.org/10.1002/jgrd.50792.

Li, S., Y. Yu, D. Sun, D. Tarpley, X. Zhan, and L. Chiu. 2014. "Evaluation of 10 Year AQUA/MODIS Land Surface Temperature with SURFRAD Observations." *International Journal of Remote Sensing* 35 (3): 830–56. https://doi.org/10.1080/01431161.2013.873149.

Li, X., S.W. Myint, Y. Zhang, C. Galletti, X. Zhang, and B.L. Turner. 2014. "Object-Based Land-Cover Classification for Metropolitan Phoenix, Arizona, Using Aerial Photography." *International Journal of Applied Earth Observation and Geoinformation* 33: 321–30. https://doi.org/10.1016/J.JAG.2014.04.018.

Li, Z.L., B.H. Tang, H. Wu, H. Ren, G. Yan, Z. Wan, I.F. Trigo, and J.A. Sobrino. 2013. "Satellite-Derived Land Surface Temperature: Current Status and Perspectives." *Remote Sensing of Environment* 131: 14–37. https://doi.org/10.1016/j.rse.2012.12.008.

Liang, X., D.P. Lettenmaier, E.F. Wood, and S.J. Burges. 1994. "A Simple Hydrologically Based Model of Land Surface Water and Energy Fluxes for GSMs." *Journal of Geophysical Research: Atmospheres* 99 (D7): 14415–28. https://doi.org/10.1029/94JD00483.

Liu, B., Z. Xie, S. Liu, Y. Zeng, R. Li, L. Wang, Y. Wang *et al*. 2021. "Optimal Water Use Strategies for Mitigating High Urban Temperatures." *Hydrology and Earth System Sciences* 25 (1): 387–400. https://doi.org/10.5194/hess-25-387-2021.

Livneh, B., T.J. Bohn, D.W. Pierce, F. Munoz-Arriola, B. Nijssen, R. Vose, D.R. Cayan, and L. Brekke. 2015. "A Spatially Comprehensive, Hydrometeorological Data set for Mexico, the U.S., and Southern Canada 1950–2013." *Scientific Data* 2. https://doi.org/10.1038/sdata.2015.42.

Livneh, B., E.A. Rosenberg, C. Lin, B. Nijssen, V. Mishra, K.M. Andreadis, E.P. Maurer, and D.P. Lettenmaier. 2013. "A Long-Term Hydrologically Based Dataset of Land Surface Fluxes and States for the Conterminous United States: Update and Extensions." *Journal of Climate* 26 (23): 9384–92. https://doi.org/10.1175/JCLI-D-12-00508.1.

Luck, M., and J. Wu. 2002. "A Gradient Analysis of Urban Landscape Pattern: A Case Study from The Phoenix Metropolitan Region, Arizona, USA." *Landscape Ecology* 17 (4): 327–39. https://doi.org/10.1023/A:1020512723753.

Martin, M.A., D. Ghent, A.C. Pires, F.M. Göttsche, J. Cermak, and J.J. Remedios. 2019. "Comprehensive In Situ Validation of Five Satellite Land Surface Temperature Data Sets over Multiple Stations and Years." *Remote Sensing* 11 (5): 479. https://doi.org/10.3390/rs11050479.

Mascaro, G. 2017. "Multiscale Spatial and Temporal Statistical Properties of Rainfall in Central Arizona." *Journal of Hydrometeorology* 18 (1): 227–45. https://doi.org/10.1175/JHM-D-16-0167.1.

Mascaro, G., E.R. Vivoni, and L.A. Méndez-Barroso. 2015. "Hyperresolution Hydrologic Modeling in a Regional Watershed and its Interpretation Using Empirical Orthogonal Functions." *Advances in Water Resources* 83: 190–206. https://doi.org/10.1016/j.advwatres.2015.05.023.

Maurer, E.P., A.W. Wood, J.C. Adam, D.P. Lettenmaier, and B. Nijssen. 2002. "A Long-Term Hydrologically Based Dataset of Land Surface Fluxes and States for the Conterminous United States." *Journal of Climate* 15 (22): 3237–51. https://doi.org/10.1175/1520-04422002)015<3237:ALTHBD>2.0.CO;2.

Mitchell, K.E., D. Lohmann, P.R. Houser, E.F. Wood, J.C. Schaake, A. Robock, A. Brian *et al*. 2004. "The Multi-institution North American Land Data Assimilation System (NLDAS): Utilizing Multiple GCIP Products and Partners in a Continental Distributed Hydrological Modeling System." *Journal of Geophysical Research: Atmospheres* 109: D07S90. http://doi.org/10.1029/2003JD003823.

Myneni, R.b., S. Hoffman, Y. Knyazikhin, J.l. Privette, J. Glassy, Y. Tian, Y. Wang *et al*. 2002. "Global Products of Vegetation Leaf Area and Fraction Absorbed PAR from Year One of MODIS Data." *Remote sensing of environment* 83 (1–2): 214–31. https://doi.org/10.1016/S0034-4257(02)00074-3.

Navarro-Estupiñan, J., A. Robles-Morua, R. Díaz-Caravantes, and E.R. Vivoni. 2019. "Heat Risk Mapping through Spatial Analysis of Remotely-Sensed Data and Socioeconomic Vulnerability in Hermosillo, México." *Urban Climate* 31: 100576. https://doi.org/10.1016/j.uclim.2019.100576.

Opalinski, N.F., A.S. Bhaskar, and D.T. Manning. 2020. "Spatial and Seasonal Response of Municipal Water Use to Weather across the Contiguous U.S." *Journal of the American Water Resources Association* 56 (1): 68–81. https://doi.org/10.1111/1752-1688.12801.

Ozdogan, M., and G. Gutman. 2008. "A New Methodology to Map Irrigated Areas Using Multi-Temporal MODIS and Ancillary Data: An Application Example in the Continental US." *Remote Sensing of Environment* 112 (9): 3520–37. https://doi.org/10.1016/J.RSE.2008.04.010.

Ozdogan, M., M. Rodell, H.K. Beaudoing, and D.L. Toll. 2010. "Simulating the Effects of Irrigation over the United States in a Land Surface Model Based on Satellite-Derived Agricultural Data." *Journal of Hydrometeorology* 11 (1): 171–84. https://doi.org/10.1175/2009JHM1116.1.

Perez-Ruiz, E.R., E.R. Vivoni, and N.P. Templeton. 2020. "Urban Land Cover Type Determines the Sensitivity of Carbon Dioxide Fluxes to Precipitation in Phoenix." *Arizona. PLOS One* 15 (2): e0228537. https://doi.org/10.1371/journal.pone.0228537.

Rushforth, R.R., and B.L. Ruddell. 2015. "The Hydro-Economic Interdependency of Cities: Virtual Water Connections of the Phoenix, Arizona Metropolitan Area." *Sustainability* 7 (7): 8522–47. https://doi.org/10.3390/su7078522.

Salamanca, F., Y. Zhang, M. Barlage, F. Chen, A. Mahalov, and S. Miao. 2018. "Evaluation of the WRF-Urban Modeling System Coupled to Noah and Noah-MP Land Surface Models over a Semiarid Urban Environment." *Journal of Geophysical Research: Atmospheres* 123 (5): 2387–408. https://doi.org/10.1002/2018JD028377.

Schaaf, C.B., F. Gao, A.H. Strahler, W. Lucht, X. Li, T. Tsang, N.C. Strugnell *et al*. 2002. "First Operational BRDF, Albedo Nadir Reflectance Products from MODIS." *Remote Sensing of Environment* 83 (1–2): 135–48. https://doi.org/10.1016/S0034-4257(02)00091-3.

Shah, H.L., T. Zhou, M. Huang, and V. Mishra. 2019. "Strong Influence of Irrigation on Water Budget and Land Surface Temperature in Indian Subcontinental River Basins." *Journal of Geophysical Research: Atmospheres* 124 (3): 1449–62. https://doi.org/10.1029/2018JD029132.

Sheppard, P.R., A.C. Comrie, G.D. Packin, K. Angersbach, and M.K. Hughes. 2002. "The Climate of the US Southwest." *Climate Research* 21 (3): 219–38. https://doi.org/10.3354/cr021219.

Sheridan, T.E., and B. Luckingham. 1990. “Phoenix: The History of a Southwestern Metropolis.” *The Journal of American History* 77 (1): 333. https://doi.org/10.2307/2078739.

Shi, H., R.F. Auch, J.E. Vogelmann, M. Feng, M. Rigge, G. Senay, and J.P. Verdin. 2018. “Case Study Comparing Multiple Irrigated Land Datasets in Arizona and Colorado, USA.” *Journal of the American Water Resources Association* 54 (2): 505–26. https://doi.org/10.1111/1752-1688.12620.

Simonit, S., J.P. Connors, J. Yoo, A. Kinzig, and C. Perrings. 2015. “The Impact of Forest Thinning on the Reliability of Water Supply in Central Arizona.” *PLoS One* 10 (4). https://doi.org/10.1371/journal.pone.0121596.

Song, J., and Z.-H. Wang. 2016. “Diurnal Changes in Urban Boundary Layer Environment Induced by Urban Greening.” *Environmental Research Letters* 11 (11): 114018. https://doi.org/10.1088/1748-9326/11/11/114018.

Song, J., Z.H. Wang, S.W. Myint, and C. Wang. 2017. “The Hysteresis Effect on Surface-Air Temperature Relationship and Its Implications to Urban Planning: An Examination in Phoenix, Arizona, USA.” *Landscape and Urban Planning* 167: 198–211. https://doi.org/10.1016/j.landurbplan.2017.06.024.

Templeton, N.P., E.R. Vivoni, Z.H. Wang, and A.P. Schreiner-McGraw. 2018. “Quantifying Water and Energy Fluxes over Different Urban Land Covers in Phoenix, Arizona.” *Journal of Geophysical Research: Atmospheres* 123 (4): 2111–28. https://doi.org/10.1002/2017JD027845.

Thenkabail, P.S., J.W. Knox, M. Ozdogan, M.K. Gumma, R.G. Congalton, Z.T. Wu, C. Milesi *et al*. 2012. “Assessing Future Risks to Agricultural Productivity, Water Resources and Food Security: How Can Remote Sensing Help?” *Photogrammetric Engineering and Remote Sensing* 78 (8): 773–82. https://pubs.er.usgs.gov/publication/70041257.

Theobald, D.M. 2014. “Development and Applications of a Comprehensive Land Use Classification and Map for the US.” *PLoS One* 9 (4): e94628. https://doi.org/10.1371/journal.pone.0094628.

Thiery, W., A.J. Visser, E.M. Fischer, M. Hauser, A.L. Hirsch, D.M. Lawrence, Q. Lejeune, E.L. Davin, and S.I. Seneviratne. 2020. “Warming of Hot Extremes Alleviated by Expanding Irrigation.” *Nature Communications* 11 (1): 1–7. https://doi.org/10.1038/s41467-019-14075-4.

Thorp, K.R., D.J. Hunsaker, K.F. Bronson, P. Andrade-Sanchez, and E.M. Barnes. 2017. “Cotton Irrigation Scheduling Using a Crop Growth Model and FAO-56 Methods: Field and Simulation Studies.” *Transactions of the American Society of Agricultural and Biological Engineers* 60 (6): 2023–39. https://doi.org/10.13031/trans.12323.

Tian, Y., C.E. Woodcock, Y. Wang, J.L. Privette, N.V. Shabanov, L. Zhou, Y. Zhang *et al*. 2002. “Multiscale Analysis and Validation of the MODIS LAI Product: I. Uncertainty Assessment.” *Remote Sensing of Environment* 83 (3): 414–30. https://doi.org/10.1016/S0034-4257(02)00047-0.

Vahmani, P., and G.A. Ban-Weiss. 2016. “Impact of Remotely Sensed Albedo and Vegetation Fraction on Simulation of Urban Climate in WRF-Urban Canopy Model: A Case Study of the Urban Heat Island in Los Angeles.” *Journal of Geophysical Research: Atmospheres* 121 (4): 1511–31. https://doi.org/10.1002/2015JD023718.

Vahmani, P., and T.S. Hogue. 2014. “Incorporating an Urban Irrigation Module into the Noah Land Surface Model Coupled with an Urban Canopy Model.” *Journal of Hydrometeorology* 15 (4): 1440–56. https://doi.org/10.1175/JHM-D-13-0121.1.

Vivoni, E.R. 2012. “Diagnosing Seasonal Vegetation Impacts on Evapotranspiration and Its Partitioning at the Catchment Scale during SMEX04–NAME.” *Journal of Hydrometeorology* 13 (5): 1631–38. https://doi.org/10.1175/JHM-D-11-0131.1.

Vivoni, E.R., M. Kindler, Z. Wang, and E.R. Perez-Ruiz. 2020. “Abiotic Mechanisms Drive Enhanced Evaporative Losses under Urban Oasis Conditions.” *Geophysical Research Letters* 47: e2020GL090123. https://doi.org/10.1029/2020GL090123.

Volo, T.J., E.R. Vivoni, C.A. Martin, S. Earl, and B.L. Ruddell. 2014. “Modelling Soil Moisture, Water Partitioning, and Plant Water Stress under Irrigated Conditions in Desert Urban Areas.” *Ecohydrology* 7 (5): 1297–313. https://doi.org/10.1002/eco.1457.

Wan, Z., Y. Zhang, Q. Zhang, and Z.L. Li. 2004. “Quality Assessment and Validation of the MODIS Global Land Surface Temperature.” *International Journal of Remote Sensing* 25 (1): 261–74. https://doi.org/10.1080/0143116031000116417.

Wang, C., Z.H. Wang, and J. Yang. 2019. “Urban Water Capacity: Irrigation for Heat Mitigation.” *Computers, Environment and Urban Systems* 78: 101397. https://doi.org/10.1016/j.compenvurbsys.2019.101397.

Wickham, J., C. Homer, J. Vogelmann, A. McKerrow, R. Mueller, N. Herold, and J. Coulston. 2014. “The Multi-Resolution Land Characteristics (MRLC) Consortium — 20 Years of Development and Integration of USA National Land Cover Data.” *Remote Sensing* 6 (8): 7424–41. https://doi.org/10.3390/rs6087424.

Xiang, T., E.R. Vivoni, and D.J. Gochis. 2014. “Seasonal Evolution of Ecohydrological Controls on Land Surface Temperature over Complex Terrain.” *Water Resources Research* 50 (5): 3852–74. https://doi.org/10.1002/2013WR014787.

Xiang, T., E.R. Vivoni, D.J. Gochis, and G. Mascaro. 2017. “On the Diurnal Cycle of Surface Energy Fluxes in the North American Monsoon Region Using the WRF-Hydro Modeling System.” *Journal of Geophysical Research: Atmospheres* 122 (17): 9024–49. https://doi.org/10.1002/2017JD026472.

Xiang, T., E.R. Vivoni, and D.J. Gochis. 2018. “Influence of Initial Soil Moisture and Vegetation Conditions on Monsoon Precipitation Events in Northwest Mexico.” *Atmosfera* 31 (1): 25–45. https://doi.org/10.20937/ATM.2018.31.01.03.

Xie, Y., T.J. Lark, J.F. Brown, and H.K. Gibbs. 2019. “Mapping Irrigated Cropland Extent across the Conterminous United States at 30 m Resolution Using a Semi-Automatic Training Approach on Google Earth Engine.” *ISPRS Journal of Photogrammetry and Remote Sensing* 155: 136–49. https://doi.org/10.1016/J.ISPRSJPRS.2019.07.005.

Yang, F., J. Yang, J. Wang, and Y. Zhu. 2014. “Assessment and Validation of MODIS and GEOV1 LAI with Ground-Measured Data and an Analysis of the Effect of Residential Area in Mixed Pixel.” *IEEE Journal of Selected Topics in Applied Earth Observations and Remote Sensing* 8 (2): 763–74. https://doi.org/10.1109/JSTARS.2014.2340452.

Yang, J., and Z.H. Wang. 2017. “Planning for a Sustainable Desert City: The Potential Water Buffering Capacity of Urban Green Infrastructure.” *Landscape and Urban Planning* 167: 339–47. https://doi.org/10.1016/j.landurbplan.2017.07.014.

Yang, Q., X. Huang, and Q. Tang. 2020. “Irrigation Cooling Effect on Land Surface Temperature across China Based on Satellite Observations.” *Science of the Total Environment* 705: 135984. https://doi.org/10.1016/j.scitotenv.2019.135984.

Yang, Y., J. Smith, L. Yang, M.L. Baeck, and G. Ni. 2019. “Regional Impacts of Urban Irrigation on Surface Heat Fluxes and Rainfall in Central Arizona.” *Journal of Geophysical Research: Atmospheres* 124: 6393–410. https://doi.org/10.1029/2018JD030213.

Yu, Y., D. Tarpley, J.L. Privette, M.D. Goldberg, M.R.V. Raja, K.Y. Vinnikov, and H. Xu. 2009. “Developing Algorithm for Operational GOES-R Land Surface Temperature Product.” *IEEE Transactions on Geoscience and Remote Sensing* 47 (3): 936–51. https://doi.org/10.1109/TGRS.2008.2006180.

Zheng, B., S.W. Myint, P.S. Thenkabail, and R.M. Aggarwal. 2015. “A support Vector Machine to Identify Irrigated Crop Types Using Time-Series Landsat NDVI Data.” *International Journal of Applied Earth Observation and Geoinformation* 34 (1): 103–12. https://doi.org/10.1016/j.jag.2014.07.002.